Invited Paper

# Overview of Raman Lidar Techniques for Air Pollution Measurements

C. Russell Philbrick[1]
Penn State University
Department of Electrical Engineering
University Park PA 16802

## ABSTRACT

Raman lidar has been demonstrated to provide vertical profiles of several of the key parameters needed for investigations of air quality. The time sequence of atmospheric profiles is most valuable for understanding the meteorological processes controlling the evolution of events and exposure associated with air pollution. The vibrational and rotational Raman lidar signals provide simultaneous profiles of meteorological data, ozone and measurements of airborne particulate matter. An operational prototype Raman lidar instrument makes use of 2nd and 4th harmonic generated laser beams of a Nd:YAG laser to provide both daytime and nighttime measurements. The Raman scatter signals from vibrational states of water vapor and nitrogen provide robust profiles of the specific humidity in the lower atmosphere. The temperature profiles are measured using the ratio of rotational Raman signals at 530 and 528 nm from the 532 nm beam of the Nd:YAG laser. In addition, the optical extinction profiles can be determined from the measured gradients in each of several molecular species scattering profiles compared to the molecular scale height. Wavelengths at 284 nm, 530 nm and 607 nm have been used routinely to determine profiles of optical extinction. The ozone profiles in the lower troposphere are measured using a DIAL analysis of the ratio of the vibrational Raman signals for nitrogen (284 nm) and oxygen (278 nm), which are on the steep side of the Hartley band of ozone. Examples from several data sets are used to demonstrate the utility of Raman lidar to describe the evolution of air pollution events. The examples presented have been selected to show the new level of understanding of air pollution events that is being gained from applications of lidar techniques.
**Keywords:** Lidar, Raman scatter, remote sensing, air pollution, optical extinction, tropospheric ozone

## 1. INTRODUCTION

Air pollution has been demonstrated to affect health, influence our activities due to changes in visibility, and is the focus of our concern for the global environment due to effects of "greenhouse gases" and increasing particle scattering albedo on the Earth's radiation balance. The two principal components of the atmosphere that have been singled out as major air pollution concerns are ozone and airborne particulate matter (PM). Airborne particulate matter has been shown to be associated with increased hospital admissions for cardiovascular disease.[1,2] Ozone is a known toxic species that causes deleterious respiratory effects, particularly causing blisters in the respiratory tract, ageing of tissue and complications for older individuals, and those with asthma and other respiratory problems.[3,4] The increase in airborne particulate matter has changed the optical properties of the atmosphere by decreasing visibility which directly affects air traffic patterns and landing frequency of commercial aircraft, and by reducing the aesthetic appreciation of our national parks.[5] The increase of emissions into the atmosphere causes two competing mechanisms which affect the energy balance that controls our global climate: 1) increased emission of chemical species that absorb infrared radiation leads to global warming due to the greenhouse effect, 2) increasing airborne particulate matter reduces the direct and indirect flux of solar radiation at the surface due to changes in the planetary albedo. Increases in optical scattering by airborne particulate matter results in reduction of global temperature, thus counteracting the increases expected from the greenhouse effect and leading to a complicated non-linear response. The increase in airborne particulate matter is principally due to combustion products from transportation and power generation.[4] The goal of present research is to assist in understanding the physical and chemical processes that result in air pollution episodes and global environment changes, so that policies can be developed that will avert severe conditions and show the best directions for action.

[1]Contact Information: crp3@psu.edu; 814-865-2975


Lidar Remote Sensing for Industry and Environment Monitoring II, Upendra N. Singh, Editor,
Proceedings of SPIE Vol. 4484 (2002) © 2002 SPIE · 0277-786X/02/$15.00

The Raman lidar described here is expected to be an important tool to gain the understanding required to predict and mitigate future air pollution episodes. Raman lidar is a robust tool that can be employed to measure a wide range of meteorological and environmental properties.[6] The most important parameters for testing our understanding of model calculations are the measured vertical profiles of ozone and particulate matter. In the past, the general approach used in developing the data to study air pollution was based upon networks of ground sites that make local *insitu* measurements. Prior investigations have suffered from the fact that little information was obtained on the vertical structure because of the expense of using aircraft and balloon platforms to obtain measurements aloft. Raman lidar can provide continuous time sequences of the vertical profiles of the key parameters in the lower atmosphere. The examples of profiles shown here demonstrate the capability for measuring the needed properties. The ozone profiles in the lower atmosphere are measured directly from the absorption in the Hartley band. The particulate mater is determined from the measurements of optical extinction and backscatter at visible and ultraviolet wavelengths. The most important meteorological parameters are temperature and water vapor. Temperature is measured from the profiles of the rotational Raman intensity. The water vapor is determined from the specific humidity measured by the ratio of the vibrational Raman radiation scattered by water vapor and molecular nitrogen. The water vapor is a particularly important tracer of the tropospheric dynamics and is the best marker of the thickness of the planetary boundary layer, which describes the dilution volume for the chemical species injected into the atmosphere. The Raman lidar techniques used to investigate air pollution events will be described in the following section. Examples from the results of several investigations will be shown to provide examples of the capability of Raman lidar to be used as a tool for studies of the physical and chemical processes active during air pollution events.

## 2. RAMAN LIDAR MEASUREMENT TECHNIQUES

Raman scattering is one of the processes that occurs when optical radiation is scattered from the molecules of the atmosphere. It is most useful because the vibrational Raman scattering provides distinct wavelength shifts for species specific vibrational energy states of the molecules and rotational Raman scattering provides signals with a wavelength dependence directly related to the atmospheric temperature.[6] Figure 1(a) shows a diagram of the vibrational and rotational energy levels that are associated with Raman scatter. When a photon scatters from a molecule, the redistribution of the charge cloud results in a virtual energy state. Most of the atmospheric molecules reside in the ground vibrational level because the vibrational excitation corresponds to relatively large energy transitions (tenths of eV for simple molecules like nitrogen and oxygen) compared to the thermal energy available. After scattering occurs, most of the events result in the return of the molecule to the ground state and the emitted photon has the energy of the initial photon plus/minus the random thermal velocity of the molecule, that is the Doppler broadening. A small fraction of the transitions (order of 0.1%) result in giving part of the photon energy to the molecule, and ending in the first vibrational level (a Stokes transition). The emitted photon energy is decreased by exactly the energy of the vibrational quanta for that molecule. For the small fraction of molecules existing in the vibrational excited level, the unlikely anti-Stokes transition is possible. The relative intensities of the scattering signals are indicated by the scattering cross-section values at 532 nm in Figure 1(b). The wavelengths of vibrational Raman back scatter signals from the molecules of the water vapor and molecular nitrogen are widely separated from the exciting laser radiation and can be easily isolated for measurement using modern filter technology and sensitive photon counting detectors.[7] The ratio of rotational Raman signals at 528 nm and 530 nm provides a measurement of atmospheric temperature.[8,9] All of the molecules of the lower atmosphere are distributed in the rotational states according the local temperature. By measuring the ratio of scattered signals at two wavelengths in this distribution, the temperature can be directly measured. In order to push the lidar measurement capability into the daylight conditions, we use the "solar blind" region of the spectrum between 260 and 300 nm. The “solar blind” region is darkened by the stratospheric ozone absorption of ultraviolet radiation. Night time measurements are made using the 660nm/607nm ($H_2O/N_2$) signal ratio from the doubled Nd:YAG laser radiation at 532 nm. Daylight measurements are obtained using the 295nm/284nm ($H_2O/N_2$) ratio from the quadruple Nd:YAG laser radiation at 266 nm. A small correction for the tropospheric ozone must be applied. That correction can be obtained from the ratio of the $O_2/N_2$ signals 278nm/284nm, and from this analysis the ozone profiles in the lower troposphere are also obtained.[10] The Raman techniques, which use ratios of the signals for measurements of water vapor and temperature, have the major advantage of removing essentially all of uncertainties, such as any requirement for knowledge of the absolute sensitivity and non-linear factors.[11] Optical extinction is measured using the gradient of the measured molecular profile compared with that expected for the density gradient.[12-16]

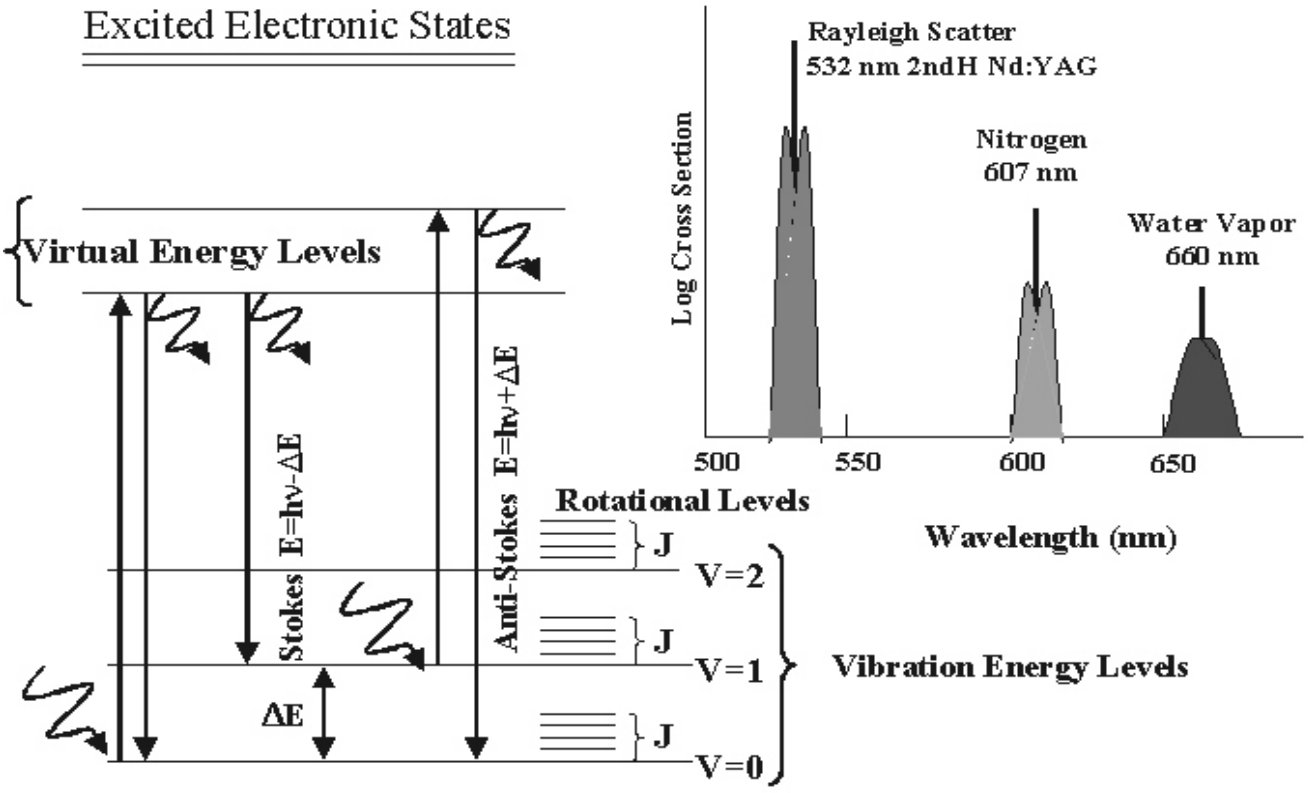


Figure 1. (a) The energy diagram of a molecule illustrates that the scattering of a photon raises the molecule to a virtual level which normally decays to ground (V=0) emitting a photon of the same energy as the incident energy, only broadened by thermal Doppler velocity. In a small fraction of cases, the return is Raman shifted to the first vibrational level (V=1), a Stokes shift. The relatively large vibrational energy ($\Delta$E) compared with thermal energy makes the anti-Stokes vibrational transition unlikely. The rotational states (J-levels) are populated by thermal excitation in both Stokes and anti-Stokes branches. (b) The relative intensities of the Stokes vibrational Raman shifts of oxygen, nitrogen and water vapor are indicated for illumination of atmospheric molecules with the 532 nm laser. The distributions of relative rotational states are indicated by envelopes of the individual lines.[6]

### 2.1. Water Vapor Measurements

The specific humidity, or water vapor mixing ratios, are determined by taking the ratio of the signals from the 1st Stokes vibrational Raman shifts for water vapor and nitrogen. The measurements are made with laser lines at visible (532 nm) and ultraviolet (266 nm) wavelengths. The visible measurements (660/607) are available at night and the ultraviolet measurements (294/284) are available day and night. The ultraviolet profiles are limited to the first 3 km because of signal loss due to the large scattering cross-section. The ultraviolet water vapor instrument calibration value has remained relatively constant for the LAPS during the past five years, however the visible sensitivity has shown significant changes, possibly due to overload the photomultiplier tube during daylight. Investigation of the stability of the instrument has shown that the variations between the meteorological balloon sonde water vapor and the lidar are about ±4%, and this is approximately the value expected due to the spatial and temporal differences.[16]

### 2.2. Ozone Measurements

The Raman vibrational 1st Stokes shifts from molecular nitrogen and oxygen are used as the sources for ozone profiles. Since the ratio of these two principal molecular constituents is constant to within 10 ppm in the lower atmosphere, any variation in the vertical profile of this ratio can be associated with the integrated absorption due to ozone.[17] The only other species that has been found to be of concern at these wavelengths is $SO_2$, which we have observed in diesel exhaust plumes.[16] Figure 2 shows the location of the Raman shifted wavelengths on the sloped side of the Hartley Band. Using

the laboratory measured cross-sections in a DIAL lidar inversion analysis, the concentrations of ozone can be calculated.[6,12] This technique eliminates the task of tuning and stabilizing the frequency and relative power of transmitted wavelengths as required for typical DIAL measurements. The fact that the nitrogen and oxygen molecules scatter a known fraction of the two Raman wavelengths in each volume element makes the technique a very robust measurement.

### 2.3. Optical Extinction Measurements

The extinction coefficient is made up of components due to absorption by chemical species and particles, and scattering by molecules and particles.[18] The Raman scatter signals from the major molecular species provide direct measurements of the optical extinction. The signal at the transmitted wavelength exhibits a profile that combines molecular and particle scattering, and it is difficult to analyze for significant properties, except cloud height. However, analysis of the Raman profiles from molecular scattering signals can provide unique vertical profiles of optical extinction. The LAPS instrument measures the optical extinction profiles from the gradients in each of the measured molecular profiles, at 607, 530 and 284 nm. The wavelength dependent optical extinction can be used to describe changes in the particle size distribution as a function of altitude for the important small particle sizes. These measurements can then be interpreted to determine the air mass parameter and atmospheric optical density. Measurements of optical extinction are based upon gradients in the molecular profiles, using the $N_2$ vibrational Raman scattering or a band of the rotational Raman lines. The calculation is easily applied to the rotational Raman signal at 530 nm because it is so close to the 532 nm transmitted wavelength that no wavelength dependence exists. By first calculating the extinction at 532 nm from the 530 nm path, it is possible to calculate the optical extinction at 607 nm without assuming a wavelength dependance for aerosol scattering.

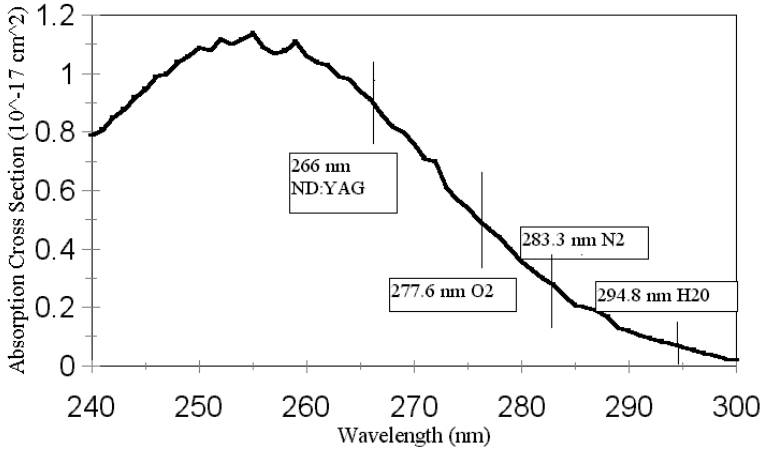


Figure 2. The absorption cross-section of the Hartley band of ozone is shown with the incident and scattered wavelengths indicated.[19]

## 3. LAPS INSTRUMENT

The LAPS lidar instrument has been developed from lessons learned during the development and use of five prior lidar instruments. The instrument was demonstrated as the first operational prototype lidar for the US Navy in 1996.[16, 20, 22] The long term goal for this instrument development is to replace most of the current balloon sonde profiling and thus enable data collection to support continuous routine measurements and meet the requirements for future meteorological data. The shipboard testing of the Lidar Atmospheric Profile Sensor (LAPS) instrument demonstrated its ability to measure the principal atmospheric properties and capability for automated operation under a wide range of meteorological conditions. The instrument measures the water vapor profile based on the vibrational Raman scattering, and the temperature profile based on the rotational Raman scattering. Profiles are currently obtained at each minute, with a vertical resolution of 75 meters from the surface to 7 km. The LAPS instrument includes several sub-systems to automate the operation and provide the real-time results. Also, the instrument includes an X-band radar which detects aircraft as they approach the beam and automatically protects a 6 degree cone angle around the beam. Table 2 lists the primary characteristics of the LAPS lidar and Table 3 lists the measurements obtained and the typical altitude range of the data products expected.

Table 2. LAPS Lidar characteristics

| | | |
|---|---|---|
| Transmitter | Continuum 9030 -- 30 Hz<br>5X Beam Expander | 600 mj @ 532 nm<br>130 mj @ 266 nm |
| Receiver | 61 cm Diameter Telescope | Fiber optic transfer |
| Detector | Seven PMT channels<br>Photon Counting | 528 and 530 nm -- Temperature<br>660 and 607 nm -- Water Vapor<br>294 and 285 nm -- Daytime Water Vapor<br>276 and 285 nm -- Raman/DIAL Ozone |
| Data System | DSP 100 MHZ | 75 meter range bins |
| Safety Radar | Marine R-70 X-Band | protects 6° cone angle around beam |

Table 3. Measurements made by the LAPS lidar instrument

| **Property** | **Measurement** | **Altitude** | **Time Resolution** |
|---|---|---|---|
| **Water Vapor** | 660/607 Raman<br>294/285 Raman | Surface to 5 km<br>Surface to 3 km | Night - 1 min.<br>Day & Night - 1 min. |
| **Temperature** | 528/530 Rot. Raman | Surface to 5 km | Night (30 min.) |
| **Ozone** | 276/285 Raman/DIAL | Surface to 2 - 3 km | Day and Night (30 min.) |
| **Optical Extinction at 530 nm** | 530 nm Rot. Raman | Surface to 5 km | Night (10 to 30 min.) |
| **Optical Extinction at 607 nm** | 607 $N_2$ - 1$^{st}$ Stokes | Surface to 5 km | Night (10 to 30 min.) |
| **Optical Extinction at 285 nm** | 285 $N_2$ - 1$^{st}$ Stokes | Surface to 3 km | Day and Night (30 min.) |

## 4. RESULTS AND EXAMPLES OF APPLICATIONS TO AIR QUALITY

The LAPS instrument uses Raman lidar techniques to simultaneously provide the profiles of water vapor, temperature, ozone and optical extinction. The goal of this paper is to introduce the measurements using examples from the recent application of the techniques to investigations of air quality. The measurement campaigns which have contributed to the present capabilities of the Raman lidar are listed in Table 4. The results presented here were obtained during the shipboard testing in 1996 on the USNS Sumner, the measurements during the Southern California Ozone Study SCOS97 and measurements from a research program referred to as the North American Research Strategy for Tropospheric Ozone - Northeast - Oxidant and Particle Study (NARSTO-NE-OPS).[21] The later program has been conducted by a consortium of universities and government laboratories and is focused on the air quality in the urban corridor extending through the northeastern states.

Table 4. Raman Lidar Measurement Campaigns

LADIMAS – RV Polarstern – Tromso, Norway to Antarctica – Oct 90-Jan 91
VOCAR – Pt Mugu CA – 1993, 1994
CASE – Wallops Island VA – Sept 1995
NARSTO-Northeast – Gettysburg PA – July 1996
USNS Sumner – Gulf of Mexico and Atlantic – Aug-Oct 1996
SCOS97 – Hesperia CA – Aug-Sept 1997
ARM and FIRE – Point Barrow AK – Feb-May 1998
NARSTO-NE-OPS – Philadelphia PA – August 1998
NARTSO-NE-OPS – Philadelphia PA – Jun-Aug 1999
NARSTO-NE-OPS – Philadelphia PA – Jun-Jul 2001

The primary measurement site is located in Philadelphia, PA. Figure 3 shows examples of profiles of water vapor, ozone and optical extinction. The water vapor profiles obtained with the LAPS instrument are shown together with measurements from a tethersonde of Millersville University (Richard Clark) and aircraft measurements form the University of Maryland (Bruce Doddridge). These daytime measurements exhibit the variations of an active convective boundary layer. The ozone profiles of the LAPS instrument and the University of Maryland aircraft are compared at night when the ozone profile is almost constant in the region of the residual boundary layer between 200 and 1700 meters. In the free troposphere, ozone patches can exist for relatively long period of time and are frequently observed to drift in the background wind. Within the thin nocturnal boundary layer, below 200-300 meters, the ozone is lost due to deposition and oxidation at the surface as well as loss from surface layer chemical processes. The optical extinction profiles are shown for wavelengths at visible and ultraviolet wavelengths. It is interesting to note that the visible wavelengths exhibit a strong correlation with water vapor content of the atmosphere, as would be expected for the hygroscopic sulfate and nitrate aerosols that are the dominate types in the eastern states. The ultraviolet extinction profile, which could represent slightly smaller particles, does not appear to correlate with the water vapor content, and may represent a non-hygroscopic particulate such as the carbonaceous or volatile organic materials. The temperature profiles are not presented here because they are less meaningful for interpretation of air quality issues. Profiles presented as time sequences of the properties are much more useful for understanding the physical and chemical processes. The results shown in Figure 4 are taken from the time period of the major air pollution episode that occurred during the summer of 1998. The measurements of the profiles of water vapor and ozone are shown for a 10 hour period. The water vapor results are shown for comparison at the same reduced resolution as the ozone, ie. a five minute time step with a thirty minute filter width. These results show the rising of the PBL during the morning hours. At 1700 UTC (1 PM local time), the elevated layer meets and mixes with the rising boundary layer. Back trajectories of the air mass show that it originated in the mid-west industrialized region. The ozone and optical extinction measurements show an interesting response to the arrival of the air mass at 1700 UTC. Based upon the apparent initiation of the air pollution event being coincident with the arrival of the air mass, we have postulated that it contained precursor chemicals that triggered the pollution episode. Tropospheric ozone is photochemically formed from chemical emissions of nitrogen oxides and volatile organic species. The possible scenario here is that since precursor chemicals can exist in the middle troposphere for periods of many hours to days and can be transported over large distances, then rapid vertical mixing transports the species into a much warmer surface layer where they can rapidly decomposed and react to form ozone. When the PBL grows to sufficient height to include a transported layer, the chemical precursors are rapidly mixed down to ground level by the daytime convective boundary layer.

Figure 5 shows an example of the measurements obtained during the shipboard testing of the Raman lidar. Out over the Atlantic, the ozone was observed above the height of the marine boundary layer and was probably transported from production sources over the continent. The UV extinction is much larger than the visible component, as expected due to the larger cross-section for scattering from small particles. Several examples of lidar results have been selected from the Southern California Ozone Studies (SCOS97) which provide a range of interesting features. One feature observed several times was a plume of polluted air ejected from the Los Angeles basin, see Figures 6, 9 and 10. The measuring site was located at Hesperia CA (at 1166 m elevation) in the high plateau at the east end of the Los Angeles basin. The results in Figure 6 show one of the best examples of the plume being lofted up over our observation site. The plume presented here, and in each of the cases observed, shows that the high values of ozone, particulate matter and water vapor are strongly coupled. When a sea breeze, or a front, pushes the air at the coastal end of the basin, then polluted air that has accumulated at eastern end of the valley pushes up the mountain passes and spills out into the high plateau. As a contrast, Figure 7 shows a typical night and early morning period with relatively stable conditions. A typical thin nighttime boundary layer is about 300 m thick and a layer of optical extinction is observed near the top of the boundary layer, this occurs where the relative humidity is a maximum and would be expected for a hygroscopic aerosol, such as a sulfate. Under these stable conditions the ozone and water vapor concentrations are usually anti-correlated. However, the ejected plumes from the Los Angeles basin are composed of increases in water vapor, ozone and optical extinction (ie. particulate matter) that are strongly correlated. Several data sets have been included to show several of the features and variations. One point worth noting is that the ozone concentrations aloft and those at the surface are rarely directly coupled, and therefore if only surface measurements are used, the constructed model may not be too realistic. The nighttime residual layer frequently contains significant quantities of ozone above the nocturnal boundary layer and this region can act as a storage reservoir for transport of additional ozone to the surface on the next day.

Figure 8 shows an interesting time sequence of the specific humidity profiles on 18 September 1997 when aircraft and rawinsonde profiles are available for comparisons with the Raman lidar profiles. The aircraft data were obtained by Prof. John Carroll of the University of California at Davis as he made a spiral around the vertically pointed lidar beam. Comparison of the aircraft and lidar data shows good agreement. The last panel in Figure 8 shows the profiles measured by a rawinsonde balloon where the line on the lidar time sequence shows the approximate altitude versus time profile. The rather striking feature observed at 1.5 km is seen to be due to the flight of the balloon through a small region that was depleted in water vapor. The gradient of the water vapor in the 2.5 to 3 km range agrees well with the water vapor measured by the lidar at the time when the balloon passed through that region. These results graphically demonstrates that a single balloon profile can mislead the observer on the actual conditions in the atmosphere.

## 5. CONCLUSIONS

Raman lidar measurements provide the key results for understanding the physical/chemical processes associated with air pollution episodes. The primary goals of the research undertaken in the environmental programs are to investigate, understand and model the physical and chemical processes important in evolution of air pollution events. By measuring the details of the species concentrations and the meteorological factors controlling transport, it is possible to identify the local and distant sources that contribute to increased concentrations of ozone and PM2.5. Additional health physics studies attempt to connect the sources of air pollution with population exposure and health effects. Finally, the results are used to develop and test models which fully predict the distribution of air pollutants to test regulatory measures. The measurement programs also provide an opportunity to improve and validate new measuring techniques needed for process monitoring.

Measurements of the variations in the profiles of optical extinction, water vapor, and ozone provide valuable insight into the evolution of pollution events. Data taken on 21 August showed a sudden increase of ozone in the planetary boundary layer when a plume, which had been transported aloft in an elevated layer from the Midwest region, was mixed into the PBL. Since low ozone levels were observed at the surface before the plume arrived and little ozone was observed inside the plume, it was suggested that this rise was due to the presence of ozone precursors transported inside the plume. The water vapor profiles show the exact timing of the pollution event, which occurred when the thickening boundary layer mixed the plume material to the surface. These measurements show, for the first time, a sequence of dynamical processes occurring in the lower atmosphere that demonstrate the importance of vertical mixing, horizontal transport, and storage of precursor materials in an elevated layer. The details revealed in the time sequences of the lidar data add a new dimension to understand the evolution of air pollution episodes. The vertical profile information and temporal variations are expected to provide the critical tests for the models under development that are expected to be the basis for future policy development. The continuous vertical profiles that can be obtained using lidar provide an important dimension for investigating the physical and chemical process of the atmosphere. Combining the Raman lidar with other measurements, such as Doppler radar, provides the complete set of parameters for testing model predictions, evaluating dynamical processes (vertical and horizontal), investigating turbidity, obtaining optical extinction profiles and describing the meteorology of the lower atmosphere with improved temporal and spatial resolution.

## 6. ACKNOWLEDGMENTS

This work is supported by the US EPA grant titled 'Investigations of Factors Determining the Occurrence of Ozone and Fine Particles in Northeastern USA,' grant number R826373. The PSU lidar development, shipboard testing, and evaluation at several field sites have been supported by the US Navy through SPAWAR Systems Division - San Diego, PMW-185, NAVOCEANO, NAWC Point Mugu, ONR, DOE, EPA, CARB, NASA and NSF. The efforts of George Allen of Harvard School of Public Health, Richard Clark of Millersville University, Russell Dickerson and Bruce Doddridge of University of Maryland, S.T. Rao of NY State Dept. of Environmental Conservation, Ted Erdman of EPA Region 3, Bill McClenny, Sharon LeDuc, Daewon Byun, and Francis Binkowski of USEPA, Jerry Lentz of Marina Photonics, and at Penn State University, William Ryan, Dan Lysak, Tom Petach, Ed Novitsky, Guangkun Li, Alexander Achey, Gregg O'Marr, Karoline Mulik, Steven Esposito, Alex Achey, Corey Slick, and Sriram Kizhakkemadam have contributed much to the success of this project.

## 7. REFERENCES


1. Magari, S.R., R. Hauser, J. Schwartz, P.L. Williams, T.J. Smith, D.C. Christiani, "Association of Heart Rate Variability with Occupational and Environmental Exposure to Particulate Air Pollution," Circulation 104, 986-991, 2001.
2. Peters, A., D.W. Dockery, J.E. Muller and M.A. Mittleman, "Increased Particulate Air Pollution and the Triggering of Myocardial Infarction," Circulation 103, 2810-2815, 2001.
3. Mauderly, Joe, Lucas Neas, and Richard Schlesinger, "PM Monitoring Needs Related to Health Effects", *Proceedings of the PM Measurements Workshop*, EPA Report No. 2, Chapel Hill, North Carolina, pp 9-14, July 1998.
4. Albritton, Daniel L., and Daniel S. Greenbaum, "Atmospheric Observations: Helping Build the Scientific Basis for Decisions Related to Airborne Particle Matter", *Proceedings of the PM Measurements Research Workshop*, EPA Report No. 1, Chapel Hill, North Carolina, pp. 1-8, July 22-23, 1998.
5. Hidy, G. M., P. M. Roth, J. M. Hales and R. Scheffe, "Oxidant Pollution And Fine Particles: Issues And Needs," NARSTO Critical Review Series, 1998, http://odysseus.owt.com/Narsto/
6. Philbrick, C.R., "Raman Lidar Measurements of Atmospheric Properties", *Atmospheric Propagation and Remote Sensing III*, SPIE Vol. 2222, 922-931, 1994.
7. Balsiger, F., and C. R. Philbrick, "Comparison of Lidar Water Vapor Measurements Using Raman Scatter at 266nm and 532 nm," in *Applications of Lidar to Current Atmos. Topics*, SPIE Proc. Vol. 2833, 231-240 1996.
8. Balsiger, F., P. A. T. Haris and C. R. Philbrick, "Lower-tropospheric Temperature Measurements Using a Rotational Raman Lidar," in *Optical Instruments for Weather Forecasting*, SPIE Proc. Vol. 2832, 53-60, 1996.
9. Haris, P.A.T., "Pure Rotational Raman Lidar for Temperature Measurements in the Lower Troposphere," PhD Thesis for Penn State University, Department of Electrical Engineering, August 1995.
10. Esposito, S.T., and C.R. Philbrick,"Raman/DIAL Technique for Ozone Measurements," *Proceeding of Nineteenth International Laser Radar Conference*, NASA/CP-1998-207671/PT1, pp 407-410, 1998.
11. Philbrick, C.R., "Raman Lidar Capability to Measure Tropospheric Properties," *Proceeding of Nineteenth International Laser Radar Conference*, NASA/CP-1998-207671/PT1, pp 289-292, 1998.
12. O'Brien, M.D., T. D. Stevens and C. R. Philbrick, "Optical Extinction from Raman Lidar Measurements," in *Optical Instruments for Weather Forecasting*, SPIE Proceedings Vol. 2832, 45-52, 1996.
13. Philbrick, C.R., M. D. O'Brien, D, B. Lysak, T. D. Stevens and F. Balsiger, "Remote Sensing by Active and Passive Optical Techniques," *NATO/AGARD Proceedings on Remote Sensing*, AGARD-CP-582, 8.1-8.9, 1996.
14. Philbrick, C.R., D.B. Lysak, Jr., M. O'Brien and D.E. Harrison, "Lidar Measurements of Atmospheric Properties," in *Proceedings of the Electromagnetic/Electro-Optics Performance Prediction and Products Symposium*, Naval Post Graduate School, Monterey CA, 385-400, June 1997.
15. Philbrick, C.R., and D.B. Lysak, Jr., "Atmospheric Optical Extinction Measured by Lidar," *Proceedings of the NATO-SET Panel Meeting on E-O Propagation*, NATO RTO-MP-1, pp.40-1 to 40-7, 1998.
16. Philbrick. C.R., and D. B. Lysak, Jr., "Optical Remote Sensing of Atmospheric Properties," *Proceedings of the Battlespace Atmospheric and Cloud Impacts on Military Operations (BACIMO)*, Air Force Research Laboratory, AFRL-VS-HA-TR-98-0103, pg 460-468, 1999.
17. Sedlacek, III, A.J., M.D. Ray and M. Wu, "Augmenting Classical DIAL with Raman-DIAL (RaDIAL)," in *Application of Lidar to Current Atmospheric Topics III*, SPIE Proc. Vol.3757, 126-139, 1999.
18. Measures, Raymond M., Laser Remote Sensing .Wiley-Interscience, New York: 1984.
19. Inn, E.C., and Y. Tanaka, "Absorption Coefficient of Ozone in the Ultraviolet and Visible Regions," J. *Optical Society*, 43, 870-873, 1953.
20. Philbrick, C.R., and D. B. Lysak, Jr., "Lidar Measurements of Meteorological Properties and Profiles of RF Refractivity," *Proceedings of the 1996 Battlespace Atmospherics Conference*, Technical Document 2938 NCCOSC RDT&E, pg 595-609, 1996.
21. Philbrick, C.R., "Investigations of Factors Determining the Occurrence of Ozone and Fine Particles in Northeastern USA," *Proceedings of Symposium on Measurement of Toxic and Related Air Pollutants*, Air &Waste Management Association, pp 248-260, 1998.
22. Philbrick, C.R. and K Mulik**,** "Application of Raman Lidar to Air Quality Measurements," *Proceedings of the SPIE Conference on Laser Radar Technology and Applications V*, pp 22-33, 2000.

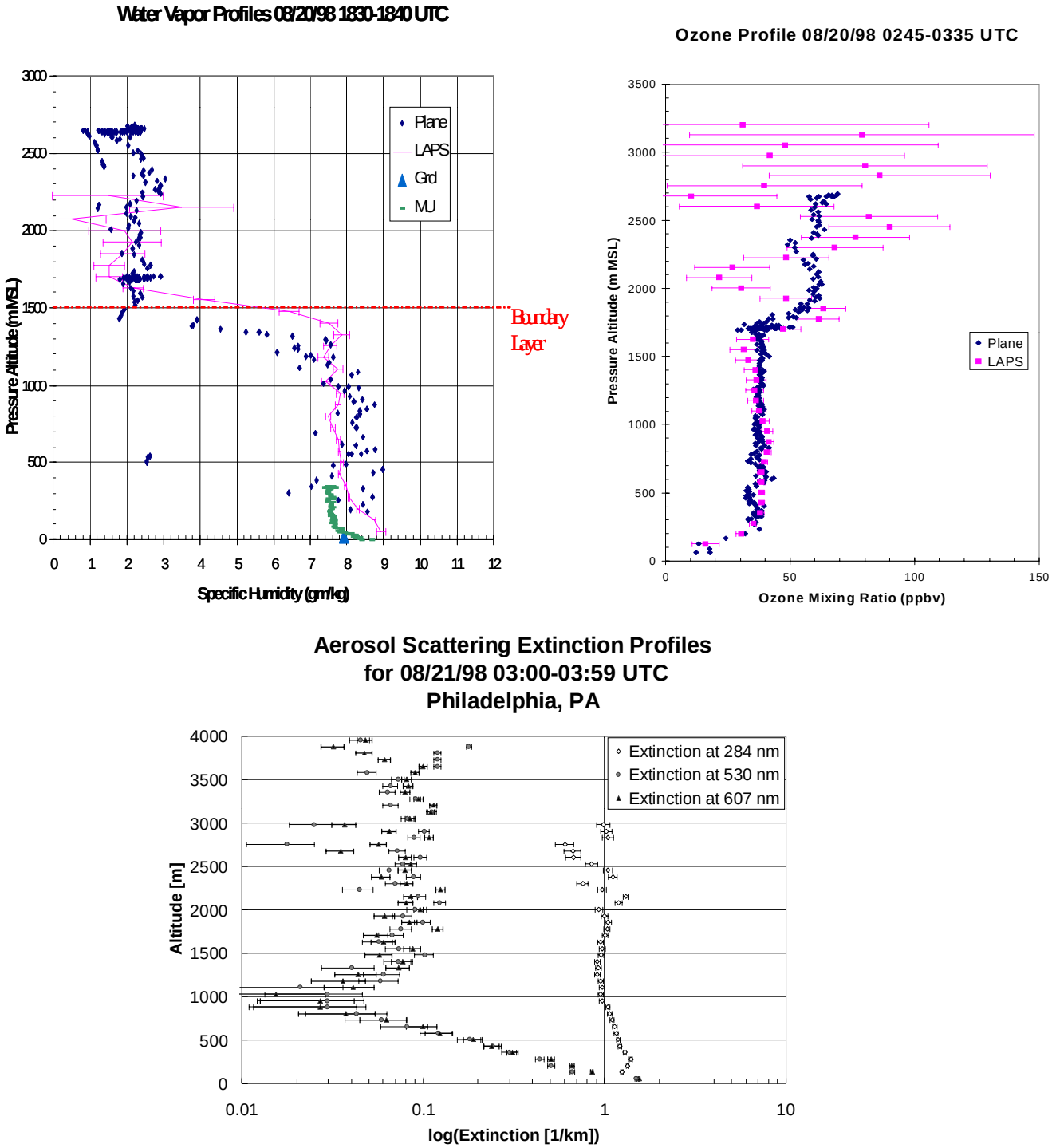


Figure 3. Examples of three sets of profiles measured by the LAPS lidar as part of the NARSTO-NE-OPS program in Philadelphia during August 1998. The water vapor measurements from LAPS lidar, the Millersville University tether sonde, and University of Maryland aircraft are compared. An ozone profile of the LAPS lidar is compared with the University of Maryland aircraft and LAPS optical extinction profiles at visible and ultraviolet wavelengths are shown.

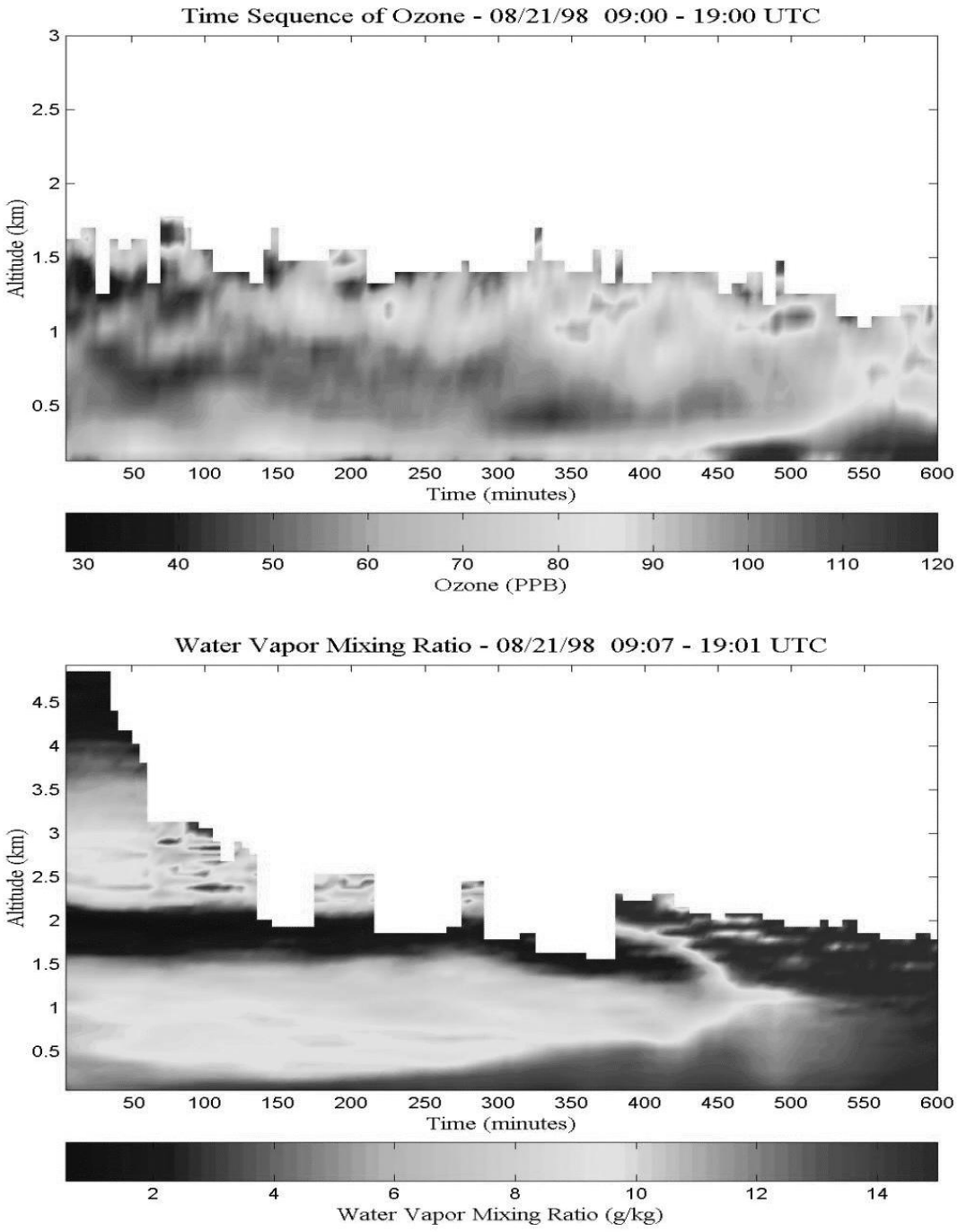


Figure 4. A 10 hour time sequence depicts the water vapor and ozone profiles for the period on 21 August 1998 that captures some interesting features of an air pollution episode. An elevated layer, which is observed to mix with the rising boundary layer at 17 UTC (1 PM local), appears to trigger an air pollution event which results in high concentrations of ozone and airborne particulate matter.

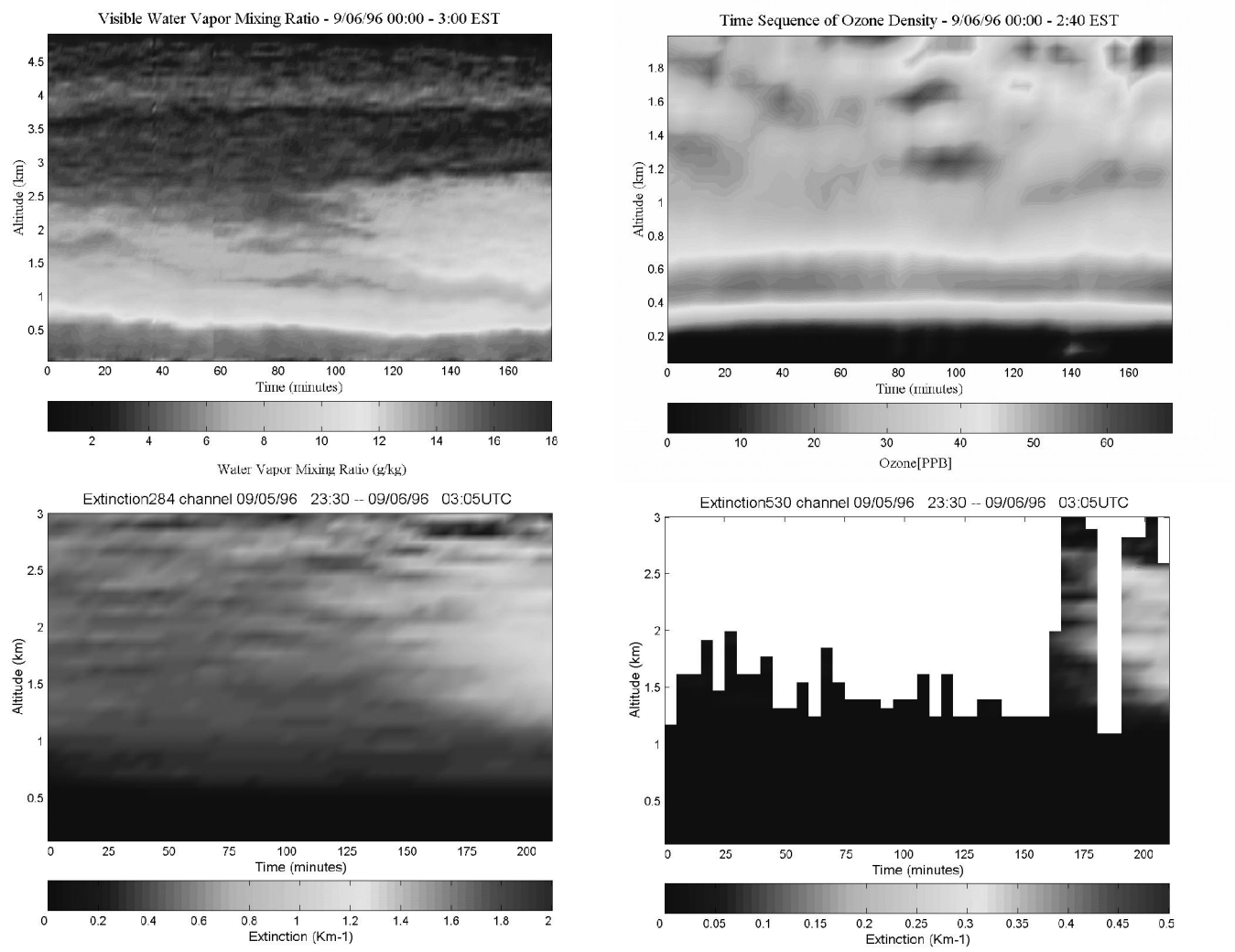


Figure 5. An example of measurements from the LAPS Navy test on the USNS Sumner on 6 September 1996 shows the water vapor, ozone and optical extinction at both visible and ultraviolet wavelengths. Note the relationship between the UV and visible extinction and the increase in optical scattering in the region of increased water vapor. The ozone is located above the marine boundary layer and is likely transported from the continent out over the Atlantic.

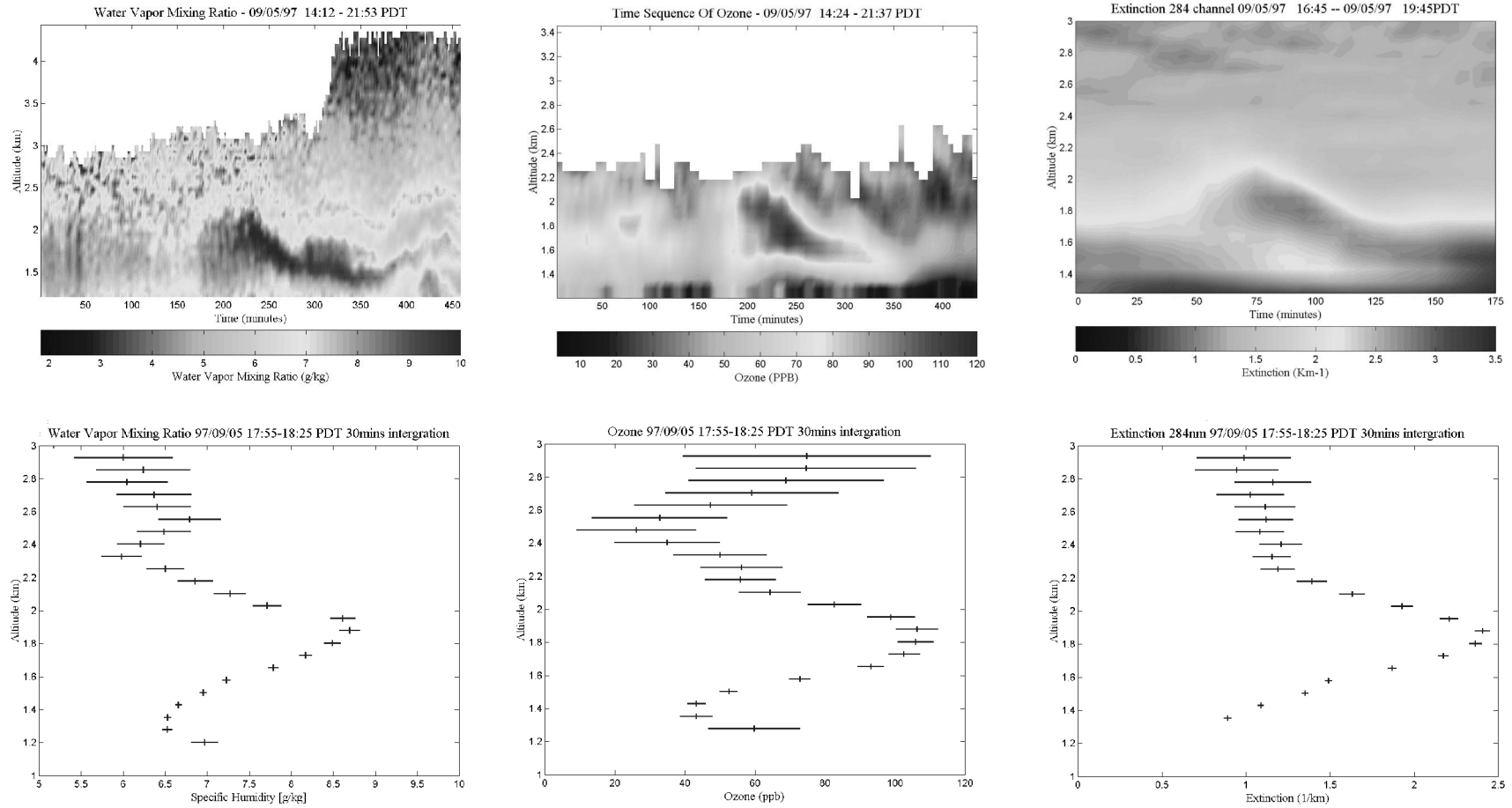


Figure 6. The water vapor, ozone and optical extinction time sequence profiles are shown during the period when a plume of polluted air from the Los Angeles basin drifts over the SCOS site at Hesperia. The water vapor plots are shown for one minute time steps with 5 minute filter and the ozone and extinction are shown with 10 minute time steps and 30 minute filter. The lower frames show the vertical profiles at the time of the passage of the plume, at 223 minutes for the water vapor, 211 minutes for the ozone, and at 70 minutes for the optical extinction.

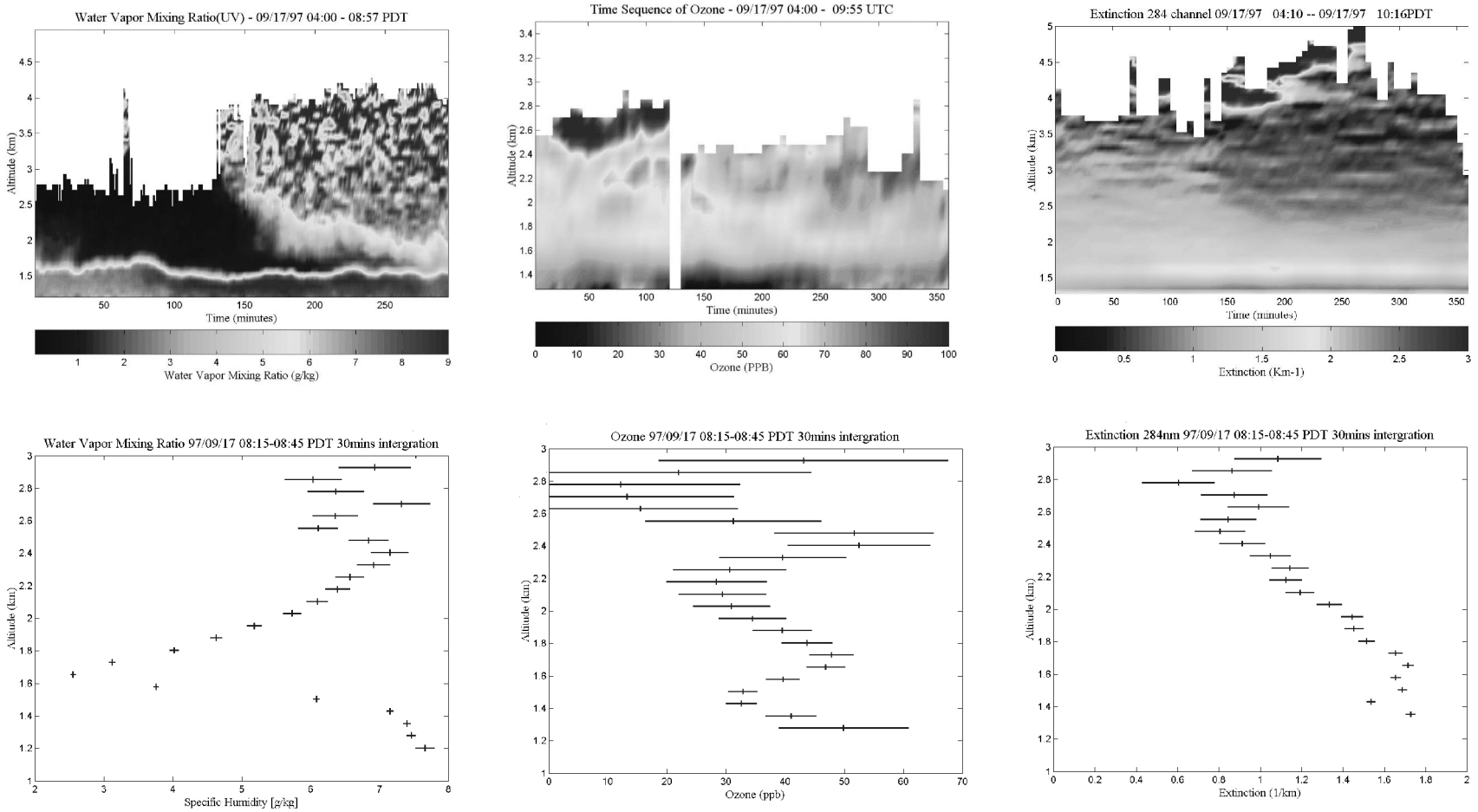


Figure 7. Comparison of the water vapor, ozone and optical extinction profiles on 17 September 1997 during the SCOS project at the Hesperia site (near 1200 m elevation) . The lower panels compare a vertical profile with the time sequence data.

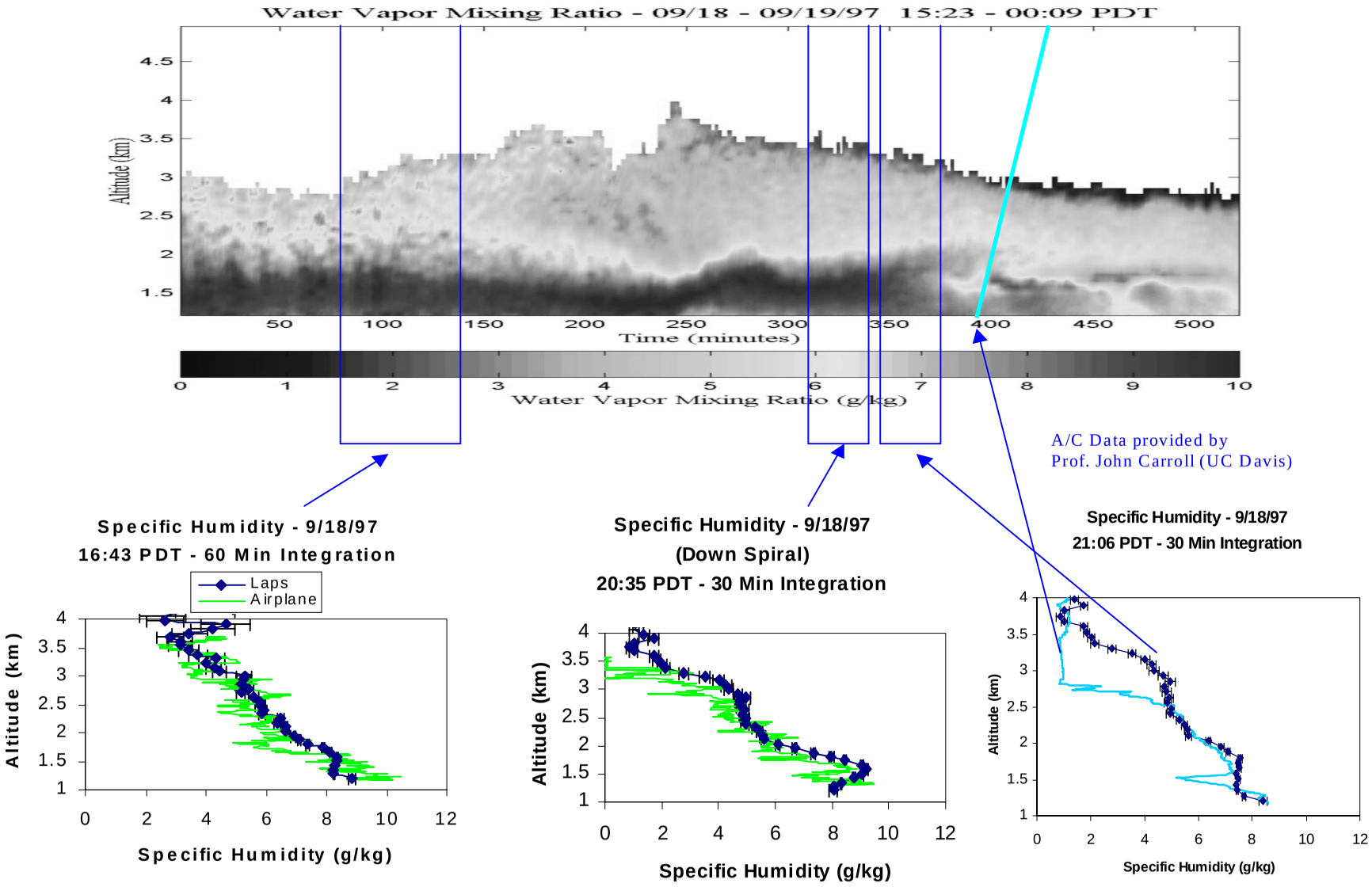


Figure 8. The time sequence of the Raman lidar profiles of water vapor are shown together with aircraft sensor measurements and a radiosonde profile for comparison. The aircraft profiles show general agreement and the differences can be correlated with features observed in the time sequences. The rawinsonde profile demonstrates the limitations of a single balloon profile compared to the complete picture provided by the lidar.

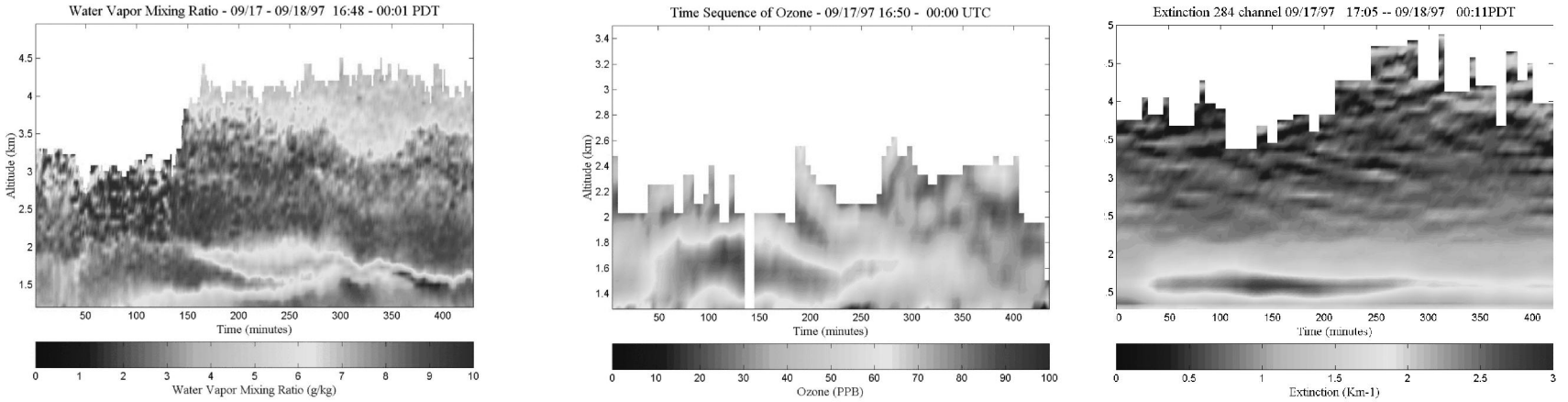


Figure 9. The water vapor, ozone and optical extinction time sequence profiles show a plume from the Los Angeles basin on 17 September 1997.

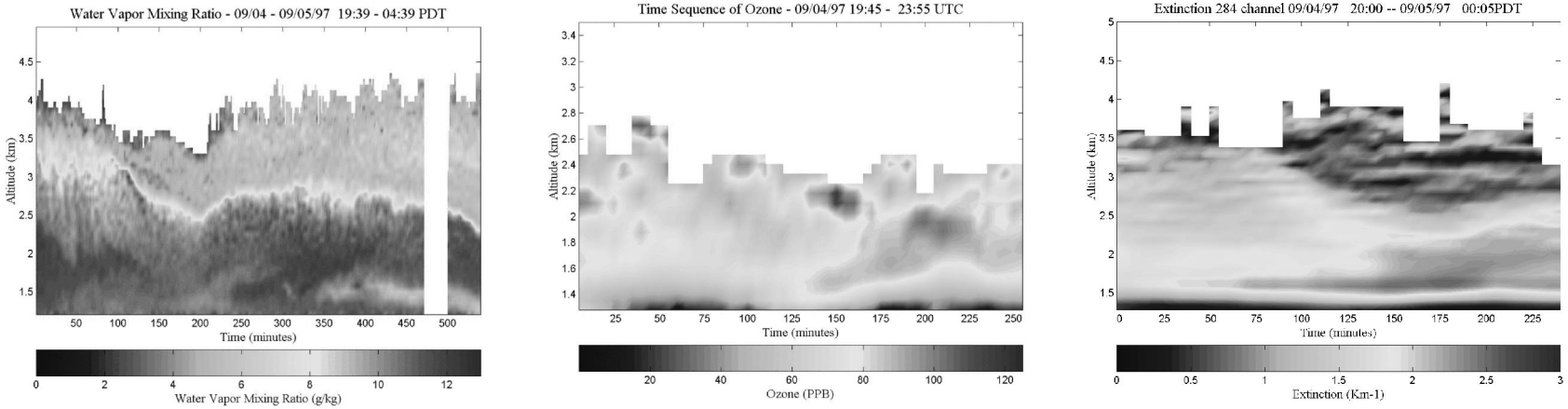


Figure 10. The water vapor, ozone and optical extinction profiles on 4 September 1997 exhibit some of the typical characteristics of the processed polluted air mass that is often blown out of the Los Angeles basin an up through the passes at the eastern end of the basin and onto the high plateau.